Volterra-Based Reconfigurable Nonlinear Equalizer for Coherent OFDM

Elias Giacoumidis, Ivan Aldaya, Mutsam A. Jarajreh, Athanasios Tsokanos, Son Thai Le, Farsheed Farjady, Yves Jaouën, Andrew D. Ellis, and Nick J. Doran

***Abstract*— A reconfigurable nonlinear equalizer (RNLE) based on inverse Volterra series transfer function is proposed for dual-polarization (DP) and multiband coherent optical orthogonal frequency-division multiplexing (OFDM) signals. It is shown that the RNLE outperforms by 2 dB the linear equalization in a 260-Gb/s DP-OFDM system at 1500 km. The RNLE improves the tolerance to inter/intraband nonlinearities, being independent on polarization tributaries, modulation format, signal bit rate, subcarrier number, and distance.**

***Index Terms*— Optical communication, coherent optical fiber transmission, nonlinear equalizer, OFDM.**

I. Introduction

COHERENT optical orthogonal frequency-division multiplexing OFDM (CO-OFDM) is a high spectral efficiency technique able to eliminate inter-symbol interference (ISI) caused by chromatic dispersion (CD) and polarization-mode dispersion (PMD) [1], [2]. Multi-band (MB) OFDM [3]–[5] is considered as a credible candidate for wavelength-division multiplexing (WDM)-based next-generation core networks. One major drawback about single-band (SB) and MB-OFDM systems is their vulnerability to fiber nonlinear effects due to the high peak-to-average power ratio (PAPR) of OFDM signals. Indeed, even in SB OFDM, due to its multi-carrier nature, four-wave mixing (FWM) occurs among OFDM subcarriers causing inter-sub-carrier interference (ICI) [4].

Consequently, nonlinearity compensation is a major issue for both SB- and MB-OFDM systems. Several digital signal processing (DSP) techniques have been investigated for the mitigation of inter/intra-channel nonlinearities. The three most prominent are the digital back propagation (DBP) [6]–[8], nonlinearity pre- and post- compensation [9] and the adaptive loading algorithms (ALAs) [10]. The main disadvantage of DBP is the extensive use of fast Fourier transform (FFT), which results in increased DSP computational complexity. The 2nd method requires a combination of pre- and post- compensation algorithms, thus providing a complex and expensive design. On the other hand, the ALAs suffer also from high DSP complexity, requiring additional negotiations between the transmitter and receiver.

Very recently, different nonlinear equalizers (NLEs) and pre-distorters based on inverse Volterra series transfer function (IVSTF) have been proposed to partially invert the dynamic nonlinear distortion induced by the transmission link. The IVSTF can be implemented in time domain (TD) [11], in frequency domain (FD) or in hybrid TD-FD [12], [13], where the CD is compensated in FD and the nonlinear distortion in the TD. NLEs have revealed improved transmission performance compared to linear equalizers for both single-carrier [13] and multi-carrier/OFDM [11] modulation formats. Additionally, IVSTF-NLEs can be generalized to operate with dual-polarization (DP) signals [12] by considering the interaction between the two polarization tributaries modelled by Manakov equation [13]. To the authors' best knowledge, a unified implementation of IVSTF-NLE capable to deal flexibly with different CO-OFDM modulations and transmission conditions has not yet been reported.

In this letter a novel reduced complexity IVSTF-based reconfigurable NLE (RNLE) is presented MB-OFDM is the worst case scenario of WDM, where the channel spacing is very small. Its equalization capabilities are evaluated in two different configurations: (a) DP SB-OFDM and (b) single polarization (SP) MB-OFDM system. In this way the polarization multiplexing and the MB multiplexing are evaluated separately. Results reveal a significant improvement in terms of Q-factor resulting from a higher tolerance to the nonlinear distortion. In DP SB-OFDM system, a neglectable influence of subcarrier number (N_{sc}) is observed, whereas for SP MB-OFDM a sensitive reduction of the inter-band spacing from 18 GHz to 8 GHz is achieved.

II. Inverse Volterra Series Transfer Function (IVSTF)-Based Flexible Nonlinear Equalizer (FNLE)

Our proposed FNLE, depicted in Fig. 1, is a generalization of the IVSTF-NLE reported in [13] to account for MB-OFDM modulation formats, as well as DP operation.

Manuscript received February 24, 2014; revised April 1, 2014; accepted April 4, 2014. Date of current version June 20, 2014. This work was supported in part by the European Commission through FP7 ICT Projects DISCUS under Grant 318137 and FOX-C under Grant 318415, in part by the Engineering and Physical Sciences Research Council under Grant EP/J017582/1-UNLOC, and in part by the Royal Society under Grant WM120035-TEST.

E. Giacoumidis, S. T. Le, F. Farjady, A. D. Ellis, and N. J. Doran are with the School of Engineering and Applied Science, Aston Institute of Photonic Technologies, Birmingham B4 7ET, U.K. (e-mail: e.giacoumidis@aston.ac.uk; let1@aston.ac.uk; f.farjady@aston.ac.uk; andrew.ellis@aston.ac.uk; n.j.doran@aston.ac.uk).

I. Aldaya is with the Department of Electrical and Computational Engineering, Instituto Tecnológico y de Estudios Superiores de Monterrey, Monterrey 64849, Mexico (e-mail: ivan.aldaya.1980@gmail.com).

M. A. Jarajreh is with the Faculty of Engineering and Environment, Northumbria University, Newcastle upon Tyne NE1 8ST, U.K. (e-mail: mutsam.jarajreh@gmail.com).

A. Tsokanos is with the School of Computing and Mathematics, Plymouth University, Plymouth PL4 8AA, U.K. (e-mail: athanasios.tsokanos@plymouth.ac.uk).

Y. Jaouën is with the Department of Communications and Electronics, Telecom Paris-Tech, Paris 75013, France (e-mail: yves.jaouen@telecom-paristech.fr).

Color versions of one or more of the figures in this letter are available online at http://ieeexplore.ieee.org.

Digital Object Identifier 10.1109/LPT.2014.2321434

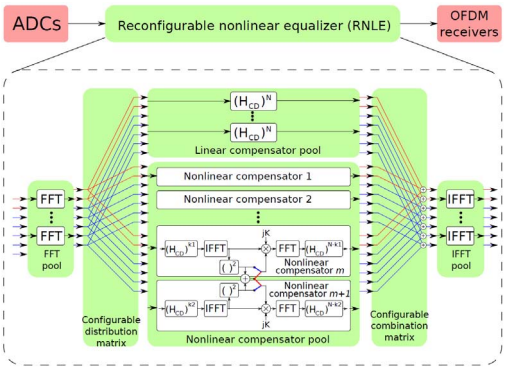

Fig. 1. Block-diagram of the proposed inverse Volterra series transfer function (IVSTF)-based reconfigurable nonlinear equalizer (RNLE).

The equalizer becomes reconfigurable (i.e. RNLE) by using the same constitutive block to compensate different sub-bands or polarizations. The blocks within the nonlinear compensator pools are linked in pairs, but they can be used flexibly for different OFDM signals. The RNLE inherits some of the features of the hybrid TD-FD implementation, such as non-frequency aliasing and simple implementation. The input signals (the DP in Case (a) and the 5 sub-bands in Case (b)) are first converted to the FD by a set of FFT modules. Once in the FD, they are distributed to the linear and nonlinear compensators by a configurable switching matrix. Each band requires only a linear compensator. On the other hand, the number of required nonlinear compensators depends on the number of OFDM sub-bands and the number of homogeneous spans in the transmission link. The interrelation between the 2-polarizations is considered by computing the total power instead of the power of each polarization independently (represented in Fig. 1 by red connections). The outputs of the linear and nonlinear compensators are combined using a configurable matrix and converted back to TD using the required number of inverse FFT (IFFT) modules. The FNLE procedure can be described from (1)–(7). Since a reduced complexity 3rd order IVSTF-FNLE is considered, the kernels $H_1(\omega, z)$ and $H_3\left(\omega_1, \omega_2, \omega-\omega_1+\omega_{2,}z\right)$ are given by,

$$H_1(\omega, z) = e^{-az/2} e^{-j\omega^2\beta_2 z/2} \tag{1}$$

$$H_3\left(\omega_1, \omega_2, \omega-\omega_1+\omega_{2,}z\right) = -\frac{j\gamma'}{4\pi^2} H_1(\omega, z) \times \frac{1-e^{-(a+j\beta_2(\omega_1-\omega)(\omega_1-\omega_2))z}}{\alpha+j\beta_2(\omega_1-\omega)(\omega_1-\omega_2)}. \tag{2}$$

where ω is the optical frequency and ω_1,ω_2 are the dummy variables acting as parameters and influence the interactions of the lightwaves at different frequency, especially the ICI interaction effects. α is the fiber loss, β_2 is the 2nd order CD parameter and γ' accounts for the effect of fiber nonlinearity averaging over the fiber birefringence ($\gamma' = 8\gamma/9$). It should be noted that higher-order kernels have been used revealing similar results. For purposes of reduced complexity and processing time the higher order kernels have not been considered here, offering ~50% reduced computational complexity compared to single-step span DBP. For an optically amplified N_{span} fiber link with L_{span} being the span length, the corresponding p-th inverse is given by the nonlinear kernels as,

$$K_1(\omega) = H_1^{-1}(\omega) = e^{j\omega^2\beta_2 N_{span} L_{span}/2} \tag{3}$$

$$K_3(\omega_1, \omega_2, \omega-\omega_1+\omega_2) = -\frac{j\gamma'}{4\pi^2} K_1(\omega) \times \frac{1-e^{-(a+j\beta_2\Delta\omega)L_{span}}}{\alpha+j\beta_2\Delta\omega} \sum_{k=1}^{N_{span}} e^{jk\beta_2 L_{span}\Delta\omega} \approx \frac{j\gamma'}{4\pi^2} \times \frac{1-e^{-\alpha L_{span}}}{\alpha} K_1(\omega) \sum_{k=1}^{N_{span}} e^{jk\beta_2 L_{span}\Delta\omega} \tag{4}$$

The corresponding compensation scheme representing (3) and (4) is applied in Fig. 1. Each nonlinear compensation stage is a realization of

$$K_{3,k}(\omega_1, \omega_2, \omega-\omega_1+\omega_2) \approx \frac{j\gamma'}{4\pi^2} \times \frac{1-e^{-\alpha L_{span}}}{\alpha} K_1(\omega) e^{jk\beta_2 L_{span}\Delta\omega} \tag{5}$$

and for the case of DP we have

$$S_{x,k1}(\omega) = \iint_{\infty}^{\infty} K_{3,k1}(\omega_1, \omega_2, \omega-\omega_1+\omega_2) \times [A_x(\omega_1)A_x^*(\omega_2)+A_y(\omega_1)A_y^*(\omega_2)] \times A_x(\omega-\omega_1+\omega_2) d\omega_1 d\omega_2 \tag{6}$$

$$S_{y,k2}(\omega) = \iint_{\infty}^{\infty} K_{3,k2}(\omega_1, \omega_2, \omega-\omega_1+\omega_2) \times [A_x(\omega_1)A_x^*(\omega_2)+A_y(\omega_1)A_y^*(\omega_2)] \times A_y(\omega-\omega_1+\omega_2) d\omega_1 d\omega_2 \tag{7}$$

where $S_{x,k1}(\omega)$ and $S_{y,k2}(\omega)$ are derived by passing the received signal of x- and y-direction through $(H_{CD})^{(k1,k2)}$, and then doing the nonlinear compensation of $jK(|.|_x^2+|.|_y^2)(.)_x$ and $jK(|.|_x^2+|.|_y^2)(.)_y$, where we multiply the received signal by a constant K related to the nonlinear distortion and the total power. This parameter varies for the particular configuration and is obtained by sweeping it to get optimum performance, which is part of the calibration of the RNLE. Finally, the residual CD is compensated passing through $(H_{CD})^{N-(k1,k2)}$.

III. Transmission System Models

The IVSTF-RNLE scheme was validated by numerical simulations carried out in a Matlab/VPI-transmission-Maker® co-simulated environment (electrical domain in Matlab and optical components with standard single-mode fiber [SSMF] in VPI). Table 1 show the link and OFDM parameters. Two transmission cases were considered: In Case (a), a DP SB-OFDM system was studied employing 16 quadrature amplitude modulation (16QAM) and 64QAM at a raw signal bit-rate of 260 Gb/s, corresponding to 200 Gb/s net signal bit-rate taking into account the different transmission overheads, i.e. the cyclic prefix (CP) in MB-OFDM and training symbols for zero-forcing (ZF) equalization in DP-OFDM, in accordance to Table 1, at 1040 km (13 spans × 80 km [N_{span} × L_{span}]). This signal bit-rate has been chosen for fair comparison with single-carrier performance reported by Liu et al. [13]. In Case (b) a SP MB-OFDM system was analyzed with 16QAM transmitting 5 sub-bands at a total raw signal bit-rate of 149.5 Gb/s over 1500 km (15 spans × 100 km [N_{span}× L_{span}]), corresponding to a net 100 Gb/s

TABLE I
TRANSCEIVER PARAMETERS

Link Parameters	OFDM Parameters
	Ideal coherent detection
$\alpha = 0.2$ dB/km	FFT-size = 256
$\beta_2 = -21.5$ ps^2/km	CP length = 10%
$\gamma = 0.0014$ m^{-1}W^{-1}	Training sequence for ZF = 6%
PMD = 0.1 ps/km$^{1/2}$	Quantization bits = 10
$NF_{EDFA} = 5.5$ dB	Clipping ratio = 13 dB
Case (a)	**Case (a)**
$L_{span} = 80$ km	$N_{sc} = 64/128/256$
$N_{span} = 13$	260 Gb/s
$G_{EDFA} = 16$ dB	16QAM/64QAM
Case (b)	**Case (b)**
$L_{span} = 100$ km	$N_{sc} = 128$
$N_{span} = 15$	149.5 Gb/s
$G_{EDFA} = 20$ dB	16QAM

Case (a): DP SB-OFDM
Case (b): SP MB-OFDM (5 sub-bands)

signal bit-rate [4]. For the generation of OFDM we employed a CP length of 10%, which in addition of virtually eliminating ISI, it relaxes the synchronization requirements of the OFDM demodulator. An Erbium-doped fiber amplifier (EDFA) was considered for optical amplification with noise figure (NF_{EDFA}) 5.5 dB and gain (G_{EDFA}) of 16 dB and 20 dB for Case (a) and Case (b), respectively. Concerning the OFDM receiver placed after the IVSTF-NLE, a ZF multiple-input multiple-output (MIMO) equalizer [14] was used for the separation of the 2 polarization components. No laser phase-noise was considered in order to evaluate only the impacts of the fiber-induced nonlinear effects. Finally, the digital-to-analogue/analogue-to-digital converter (DAC/ADC) clipping ratio and quantization were taken into account and set to 13 dB and 10-bits, respectively, which has negligible impact on OFDM performance for subcarrier number >32 [4], [5].

In order to obtain the optimum Q-factor, the constant K was swept achieving a value [13] (since we always lock the received signal power to a specific value to reach the sensitivity of the receiver).

IV. NONLINEARITY COMPENSATION IN DUAL-POLARIZATION (DP) CO-OFDM SIGNALS

Initially, the proposed RNLE has been evaluated in a DP SB-OFDM configuration as described in Case (a). In Fig. 2 the Q-factor is plotted against the launched optical power (LOP) for 16QAM system at 260 Gb/s and 1040 km with different N_{sc}. By comparing the optimum Q with and without RNLE, a performance improvement of $\sim$2 dB is observed. Note that the intra-band nonlinearities reduction using the RNLE is quasi-independent of the N_{sc}. This occurs due to the small PAPR difference among high N_{sc} (typically >32) resulting to similar amounts of nonlinearity compensation In Fig. 3, the received constellation diagrams for the 16QAM format (N_{sc}=128) are illustrated for x polarization revealing the improvement when the RNLE is applied. In Fig. 4, the Q is plotted against LOP for 16QAM and 64QAM DP SB-OFDM (N_{sc}=128) having 35 and 25 GHz of bandwidth, respectively. For the two modulation formats, similar performance improvements are observed demonstrating that the intra-band nonlinearities reduction using the RNLE is equivalent.

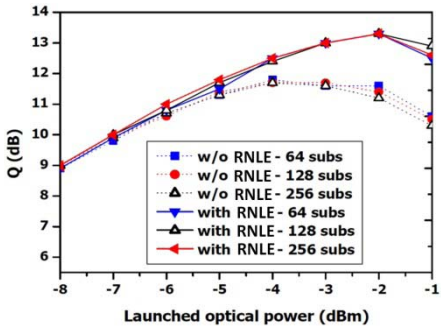

Fig. 2. Q vs. launched optical power (LOP) with and without (w/o) RNLE for 260 Gb/s 16QAM DP SB-OFDM using 64, 128 and 256 subcarriers at 1040 km.

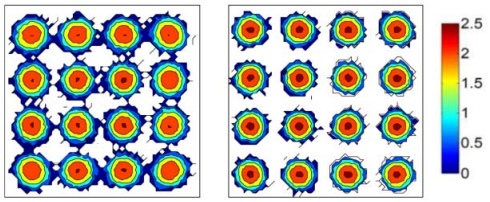

Fig. 3. Received constellations for 16QAM DP SB-OFDM with N_{sc} =128, after (a) linear and (b) nonlinear equalization at LOP of -1 dBm.

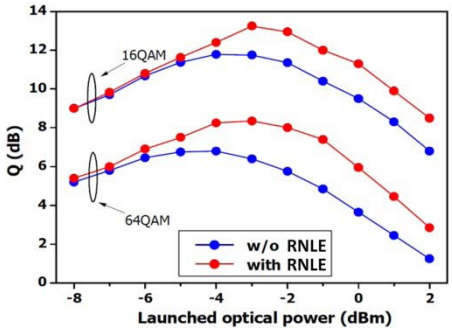

Fig. 4. Q vs. LOP with and without RNLE for a 16QAM/64QAM DP SB-OFDM (N_{sc}=128) 260 Gb/s at 1040 km.

V. NONLINEARITY COMPENSATION IN MULTI-BAND (MB) CO-OFDM SIGNALS

In order to analyze the performance of the RNLE for MB approach, in Case (b), a MB-OFDM signal with 5 sub-bands was transmitted. For the sake of simplicity of performance evaluation, a SP OFDM system has been considered. The middle sub-band was centered at 1552.93 nm. The impact of the inter-band interference was analyzed varying the inter-band frequency separation. In Fig. 5, the Q-factor in terms of the LOP is shown for different separation frequencies, with and without RNLE. The optimal LOP per sub-band value in absence of nonlinear equalization is about -7 dBm. We pointed out that the optimum LOP is increased >1 dB when RNLE is applied. As expected, the higher frequency sub-band spacing we have, the better performance is achieved for both cases, as it can be appreciated in Fig. 5.

The optimal Q-factors in term of sub-band spacing are plotted in Fig. 6 for both linear and nonlinear equalization. A $\sim$0.9 dB improvement for the Q-factor is observed in

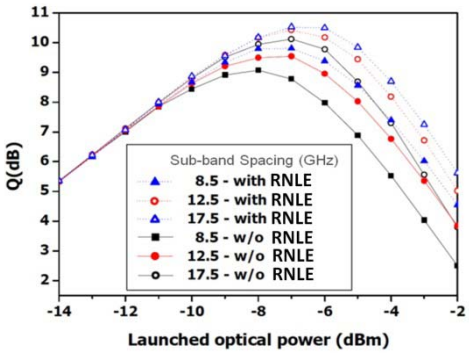

Fig. 5. Q vs. LOP per sub-band spacing with and without RNLE for a 149.5 Gb/s OFDM system (N_{sc}=128) at 1500 km.

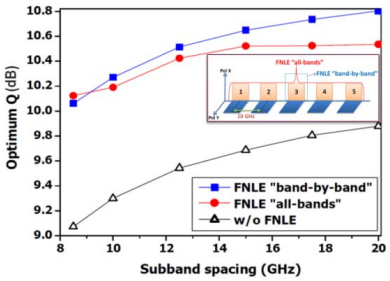

Fig. 6. Optimum Q vs. sub-band spacing using "band-by-band", "all-bands" (see inset) with and without RNLE for 149.5 Gb/s 16QAM MB (5 sub-bands)-OFDM system (N_{sc}=128) at 1500 km.

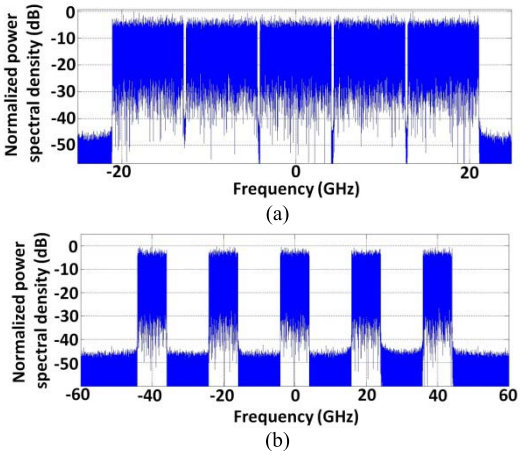

Fig. 7. Received spectrum for 149.5 Gb/s 16QAM MB (5 sub-bands)-OFDM (B2B) with sub-band spacing of (a) 8.5 GHz and (b) 20 GHz.

linear equalization case, which had previously explained by the reduction of the out-of-band FWM contributions [4], [5]. The RNLE is supposed to operate "band-by-band", processing each band separately, so reducing the computation cost. However for benchmark, the results processing "all-bands" together have also been included (see inset of Fig. 6 a schematic diagram with 5 DP sub-bands). Fig. 6 reveals that "band-by-band" outperforms "all-bands" for the entire range of sub-band spacing. This can be explained by noting that "band-by-band" RNLE compensates more accurately intra-band nonlinearities. Therefore, only when the inter-bands nonlinear effects get more significant, "all-bands" RNLE shows better performance.

In Fig. 7, the received spectrum for 149.5 Gb/s 16QAM MB-OFDM is depicted for back-to-back (B2B) with sub-band spacing of (a) 8.5 GHz and (b) 20 GHz. Finally, it should be mentioned that the "band-by-band" approach offers ~20% reduction in computational complexity compared to "all-bands".

VI. Conclusion

We proposed a reduced complexity IVSTF-RNLE to be able to process both single- and multi-bands as well as single- or dual-polarization OFDM signals. We have demonstrated that the RNLE outperforms by 2 dB the linear equalization in a 260 Gb/s DP-OFDM system at 1500 km. The RNLE has also shown to be effective for MB-OFDM systems, allowing reduction of inter-band spacing and therefore improving the spectral efficiency. Moreover, RNLE improvement over linear equalization proved to be independent from polarization tributaries, modulation format, signal bit-rate, subcarrier number and transmission distance. Given the importance of the aforementioned statements for practical WDM architecture design, experimental verifications of the statements in IVSTF-based coherent MB-OFDM have been pledged.

References

[1] S. L. Jansen, I. Morita, T. C. W. Schenk, N. Takeda, and H. Tanaka, "Coherent optical 25.8-Gb/s OFDM transmission over 4160-km SSMF," *J. Lightw. Technol.*, vol. 26, no. 1, pp. 6–15, Jan. 1, 2008.

[2] W. Shieh, H. Bao, and Y. Tang, "Coherent optical OFDM: Theory and design," *Opt. Exp.*, vol. 16, no. 2, pp. 841–859, 2008.

[3] J. Karaki *et al.*, "Dual-polarization multi-band OFDM versus single-carrier DP-QPSK for 100 Gbps long-haul WDM transmission over legacy infrastructure," in *Proc. 38th ECOC*, 2012, paper P4.17.

[4] E. Giacoumidis *et al.*, "100 Gb/s coherent optical polarization multiplexed multi-band-OFDM (MB-OFDM) transmission for long-haul applications," in *Proc. 14th ICTON*, 2012, paper We.B1.2.

[5] J. Karaki *et al.*, "Dual-polarization multi-band OFDM versus single-carrier DP-QPSK for 100 Gb/s long-haul WDM transmission over legacy infrastructure," *Opt. Exp.*, vol. 21, no. 14, pp. 16982–16991, 2013.

[6] D. Rafique and A. D. Ellis, "Various nonlinearity mitigation techniques employing optical and electronic approaches," *IEEE Photon. Technol. Lett.*, vol. 23, no. 23, pp. 1838–1840, Dec. 1, 2011.

[7] G. Gao, X. Chen, and W. Shieh, "Limitation of fiber nonlinearity compensation using digital back propagation in the presence of PMD," in *Proc. OFC/NFOEC*, 2012, paper OM3A.5.

[8] G. Gao, J. Zhang, and W. Gu, "Analytical evaluation of practical DBP-based intra-channel nonlinearity compensators," *IEEE Photon. Technol. Lett.*, vol. 25, no. 8, pp. 717–720, Apr. 15, 2013.

[9] A. J. Lowery, "Fiber nonlinearity pre- and post-compensation for long-haul optical links using OFDM," *Opt. Exp.*, vol. 15, no. 20, pp. 12965–12970, 2007.

[10] E. Giacoumidis, A. Kavatzikidis, A. Tsokanos, J. M. Tang, and I. Tomkos, "Adaptive loading algorithms for IMDD optical OFDM PON systems using directly modulated lasers," *IEEE/OSA J. Opt. Commun. Netw.*, vol. 4, no. 10, pp. 769–778, Oct. 2012.

[11] J. Pan and C.-H. Cheng, "Nonlinear electrical compensation for the coherent optical OFDM system," *J. Lightw. Technol.*, vol. 29, no. 2, pp. 215–221, Jan. 15, 2011.

[12] F. P. Guiomar, J. D. Reis, A. L. Teixeira, and A. N. Pinto, "Digital postcompensation using Volterra series transfer function," *IEEE Photon. Technol. Lett.*, vol. 23, no. 19, pp. 1412–1414, Oct. 1, 2011.

[13] L. Liu *et al.*, "Intrachannel nonlinearity compensation by inverse Volterra series transfer function," *J. Lightw. Technol.*, vol. 30, no. 3, pp. 310–316, Feb. 1, 2012.

[14] S. L. Jansen, I. Morita, T. C. Schenk, and H. Tanaka, "Long-haul transmission of 16×52.5 Gbits/s polarization-division-multiplexed OFDM enabled by MIMO processing (Invited)," *J. Opt. Netw.*, vol. 7, no. 2, pp. 173–182, 2008.